

A Model for the Dissipative Conductance in Fractional Quantum Hall States

N. d'Ambrumenil¹, B.I. Halperin² and R.H. Morf³

¹*Physics Department, University of Warwick, Coventry CV4 7AL, United Kingdom*

²*Physics Department, Harvard University, Cambridge, Massachusetts 02138, USA*

³*Paul Scherrer Institute, CH-5232 Villigen, Switzerland*

(Dated: December 1, 2021)

We present a model of dissipative transport in the fractional quantum Hall regime. Our model takes account of tunneling through saddle points in the effective potential for excitations created by impurities. We predict the temperature range over which activated behavior is observed and explain why this range nearly always corresponds to around a factor two in temperature in both integer quantum Hall and fractional quantum Hall systems. We identify the ratio of the gap observed in the activated behavior and the temperature of the inflection point in the Arrhenius plot as an important diagnostic for determining the importance of tunneling in real samples.

PACS numbers: 73.43.Cd, 73.21.-b, 73.43.Jn, 73.43.Lp

The energy gap and an incompressible ground state are essential components of all quantum Hall systems [1, 2]. Estimates of this gap have usually been found by fitting the temperature dependence of the longitudinal resistance of the highest mobility samples to the standard Arrhenius form [3–5]. However, progress towards an understanding of how the measured activation gap relates to the intrinsic gap has been held up by the lack of a detailed microscopic model of the effect of disorder on the dissipative transport.

The Arrhenius form, $\sigma = \sigma_0 e^{-\Delta/2T}$, is found only over a small range in temperature and the estimates of the gap are lower than theoretical expectations [3, 4, 6, 7]. Where it has been possible to extract estimates, σ_0 has generally been lower by around a factor of 2 than the predicted $2(qe)^2/h$ per square [8], where qe is the charge carried by the quasiparticles (QPs) or quasiholes (QHs) [9, 10].

The gap Δ extracted from experiments has often been interpreted as a zero-temperature mobility gap. Specifically, this equates Δ to the energy necessary to create a pair of separated oppositely charged quasiparticles in presumably well-defined extended single-quasiparticle states, which can then carry charge across the system [5, 11–13]. Here, however, we advance a different picture of thermally activated transport in a quantized Hall state in a modulation doped sample. Our approach generalizes the model of [8] to include the effect of thermally assisted tunneling and to account for the compressible screening regions [14, 15] which are nucleated when the gap is smaller than the unscreened potential due to ionized donors. The conductance measurements are controlled by the saddle-point gap energy, Δ_s , which is the energy required to excite excitations at a saddle point in this potential. The presence of screening regions means that Δ_s will normally be significantly less than the gap in ideal homogeneous incompressible systems, Δ_h , studied using exact diagonalizations, by an amount which is not the result of a simple broadening of levels, Γ [4, 11], and

with no simple connection to the zero field mobility [7].

Our model explains why activated behavior is normally only seen over a small regime in temperature with a factor of around two between the highest and lowest temperatures and predicts that the prefactor, σ_0 , of the Arrhenius form is reduced from its “ideal” value of $2(qe)^2/h$. We show that the gap, Δ_i , obtained from the Arrhenius plots, and the temperature range (in units of Δ_i), over which activated behavior is observed, can be used to estimate Δ_s . We find $\Delta_s/\Delta_h \approx 0.55$ for the strongest lowest Landau level (LL) states of [4] and $\Delta_s/\Delta_h \approx 0.4$, for the strongest state at $\nu = 5/2$ of [5].

The samples studied experimentally typically have the donor ions in layer(s) set back from the 2DEG. The set-back distance, d , sets the length scale for the potential fluctuations in the electron gas created by the ionized donors. In most samples and at the filling fractions and densities involved, $d \gtrsim \ell_q = \ell_0/\sqrt{q}$. Here ℓ_q is the effective magnetic length of the QP of QH, and $\ell_0 = \sqrt{\hbar/eB}$. Modeling of the positioning of the ions in the donor layers suggests that Δ_h is smaller than the unscreened impurity potential, and predicts that the system breaks up into regions of incompressible fluid separating compressible regions containing excitations, which partially screen the impurity potential [15, 16]. The quantized Hall conductance of the system is then the response of the percolating regions of incompressible fluid.

When $\ell_q \ll d$, and in the absence of screening regions, the dissipative response near the center of the quantum Hall plateau is due to the transfer of thermal excitations across saddle points in the energy landscape set up by the ionized donors [8]. Each saddle point acts as a resistor in two separate resistor networks. In one, a saddle connects together the p-type regions (QH-rich) and in the other it connects the n-type (QP-rich) regions. The conductance in each case is given by $(qe)^2 h^{-1} \exp(-E_s^{h,p}/kT)$, where E_s^h and E_s^p are the heights of the saddle point for QHs and QPs with $E_s^h + E_s^p = \Delta_s$. If the fluctuations of the impurity potential are symmetrically distributed about

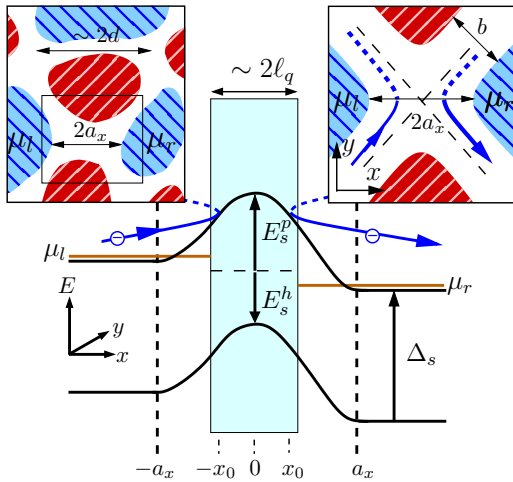


Figure 1. Band alignment and particle flow across a typical saddle point. Upper left: Break-up of a quantum Hall system. Incompressible fluid at filling fraction ν (white background) separates compressible regions in which QPs (dark diagonals on lighter shading) and QHs (light diagonals on darker shading) are nucleated [16]. Upper Right: Tunnelling of a QP through the saddle point from an equipotential line about the left region (chemical potential μ_l) to one about the right. Main figure: Energy band alignment. For QP excitations with energies $E < E_s^p$, the transmission probability is significant if the point of closest approach to the saddle point, x_0 , lies within a zone of width $\sim 2\ell_q$ about the saddle point. Potential variations in the incompressible region exceeding Δ_s are not possible. They would simply nucleate carriers and reduce the size of the incompressible region.

the mean, Dykhne's theorem [17] gives that the logarithm of the conductance of each network is the average of the logarithm of the conductance at each node and gives an overall response of $2(qe)^2 h^{-1} \exp(-\Delta_s/2kT)$.

If ℓ_q becomes comparable to d or a_x , where $2a_x$ is the width of the incompressible region at a saddle (see Fig 1), the main dissipative process still involves carriers crossing saddle points, but now there may be significant tunneling across the saddle point. There is then a range of temperatures in which the response appears activated, with an activation energy reduced from E_s by an amount which depends on a_x/ℓ_q but not on temperature.

Excitations follow the classical trajectories except in the neighborhood of a saddle point. Assuming fast equilibration in the localized regions [8, 18], the conductance of the saddle point for the transport of QPs (taken here to be moving in the x direction) is given by

$$\sigma = \frac{(qe)^2}{h} \frac{1}{kT} \int_0^{\Delta_s} dE \mathcal{T}(E - E_s) e^{-E/kT}, \quad (1)$$

where E_s is the height of the saddle point, $\mathcal{T}(E - E_s)$ is the probability that a QP with energy E is transmitted across the saddle point and Δ_s is the energy required to excite a QP or QH at a saddle point. When $\ell_q \ll a_x$, we

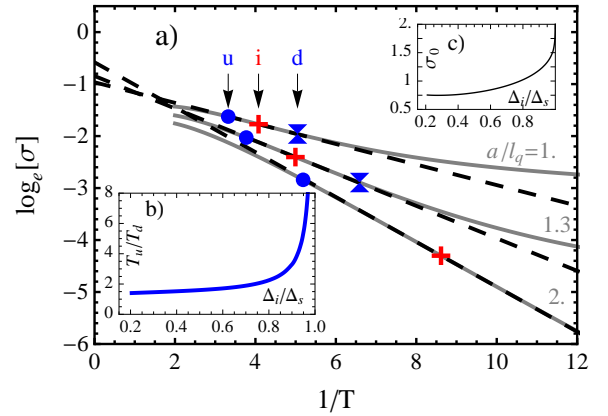


Figure 2. a) $\log_e \sigma$ vs $1/T$ for different values of a/ℓ_q (a is the typical saddle-point width). The estimated activation gap Δ_i (in units of the saddle-point gap Δ_s) is twice the maximum value of the slope (dashed line) drawn at the inflection points at temperatures T_i (crosses). $\Delta_i/\Delta_s = 0.4, 0.63$ and 0.86 for the illustrative values of a/ℓ_q . $\log_e \sigma$ appears linear in $1/T$ between T_u (disks) and T_d (hourglasses). At T_u and T_d , the slope is 95% of its value at T_i . The ratio T_u/T_d is shown in b) as a function of Δ_i/Δ_s . c) The prefactor of the activated behavior, estimated from the extrapolation of the linear region to $1/T = 0$, as a function of Δ_i .

have $\mathcal{T} = 0$ or 1, according to whether E is smaller or larger than E_s , and we recover the result of [8].

The tunneling probability, \mathcal{T} , can be computed exactly in the special case of noninteracting particles when the potential energy near the saddle is $W = E_s - U_x x^2 + U_y y^2$ [19]. Provided that $U_{x,y}/m\omega_c^2 \approx (\ell_q/a_{x,y})^2/2 < 1$, $\mathcal{T}(E - E_s) = 1/(1 + e^{-\pi(E - E_s)/(\ell_q^2 \sqrt{U_x U_y})})$, and the exponent in the denominator is given correctly by the WKB approximation. Here ω_c is the cyclotron frequency. Assuming that this form for \mathcal{T} is valid for arbitrary saddle-point potentials, we have computed the exponential factor within the WKB approximation and hence the average of $\log_e \sigma$ for different (symmetric) distributions of saddle-point heights and for different potentials. The results are not sensitive to the exact form assumed for the potential or the distribution of saddle-point heights and widths, provided these are symmetrically distributed about their mean values. The principal role of interactions is to set the energy scale, Δ_s . We ignore additional interaction effects arising from the non-Fermionic nature of the excitations which are thought to be small [20].

Figure 2a shows $\log_e \sigma$ as a function of $1/T$ for different values of the average width, a . The saddle points are described by $W = E_s - U_x x^2 + U_y y^2$, with $\sqrt{U_x U_y} = \Delta_s/2a^2$, and E_s distributed evenly between 0 and Δ_s . Approximately linear dependence of the form $\log_e \sigma \sim -\Delta_i/2T$ is observed between T_d and T_u , which we take to be the temperatures at which the gradient is within 5% of its maximum value. Δ_i is defined as twice the slope of the tangent drawn at the inflection point at temperature

T_i . For $T < T_d$, the response is dominated by activation energies lower than Δ_i but which depend on temperature. For $T > T_u$, σ is thermally activated but less than an Arrhenius law predicts, because of the upper limit in (1). (Excitations with energy above Δ_s are minority carriers localized in the adjacent puddle and do not contribute to transport). An estimate of the ratio T_u/T_d is shown in Fig 2b as a function of Δ_i/Δ_s . Except when $\Delta_i \gtrsim 0.85\Delta_s$, the ratio is around two or less. This is in line with experimental observations [3, 4, 6, 7], which also find $\log_e \sigma \sim -\Delta_i/2T$ over a temperature range with $T_u/T_d \lesssim 2$.

Figure 2c shows the prefactor of the apparent activated behavior as a function of Δ_i/Δ_s . For $\Delta_i \lesssim 0.85\Delta_s$, the prefactor is between 0.8 and 1.25 in units of $(qe)^2/h$ and only approaches the value two, predicted in [8], when the effects of tunneling are small ($\Delta_i/\Delta_s \gtrsim 0.95$). The rapid drop of σ_0 , as Δ_i/Δ_s is reduced from one, explains why σ_0 has been reported to lie between 0.8 and 1.1 [9] with only a few datapoints (mostly at $\nu = 4/3$ close to a spin transition) falling below this region [10]. However, the use of the prefactor obtained from observation is not easy, as it involves exponentiation of a value obtained by extrapolating to the limit $1/T \rightarrow 0$, and may not be a reliable measure of the tunneling effect.

The extent of thermally assisted tunneling in actual samples can be estimated from Δ_i/T_i . While the effect is controlled in our model by the ratio a/ℓ_q , the ratio Δ_i/T_i is directly accessible experimentally. We have estimated Δ_i/T_i for sample A of [4] (which has $d = 80\text{nm}$) both by looking for the inflection point and from the values for T_u and T_d (our model gives $1/T_i$ at around $0.6/T_u + 0.4/T_d$). From the dependence of Δ_i/Δ_s as a function of Δ_i/T_i , which is shown in Fig 3, we obtain the estimates of Δ_s given in the inset table. We also include estimates for the average saddle-point width, a , and the gap for ideal homogeneous systems, Δ_h [6, 21].

Two striking features of the estimates in Fig 3 are that the typical saddle-point widths a do not vary much between filling fractions $1/3$ and $4/9$ for the given sample and that the saddle-point gaps, Δ_s , are consistently a factor around two less than the values predicted for homogeneous systems, Δ_h . Given that the width of the incompressible strips, b , is not expected to vary significantly for filling fractions in the hierarchy, we should also expect a to be approximately constant. b is determined by the electrostatic potential difference, $\delta\phi$, between the two sides of the incompressible region, set up by the charge redistribution needed to pin the charge density to its incompressible value. If the electrostatic energy gain from transferring a QP across the region exceeds the gap energy, QPs and QHs will be nucleated on both sides. The width of the strip is fixed by the condition $e\delta\phi = \Delta_s/q$. Δ_s/q is the discontinuity in chemical potential for electrons, which is expected to be nearly constant (in units of $e^2/\epsilon\ell_0$) for hierarchy states [22]. This leaves only a weak

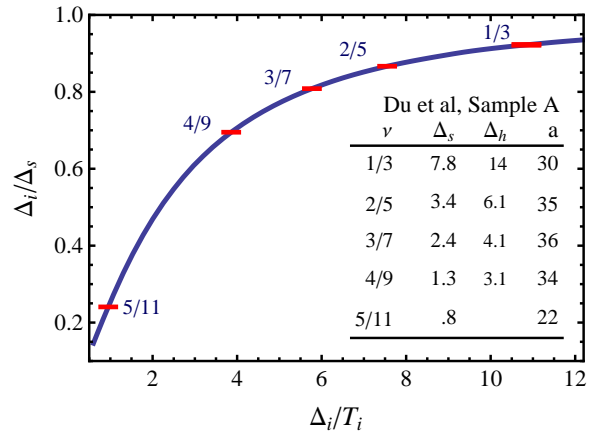


Figure 3. The ratio of the apparent gap to the saddle-point gap, Δ_i/Δ_s , as a function of Δ_i/T_i . Points are placed on the curve at the values of Δ_i/T_i for sample A of [4]. This allows us to estimate Δ_i/Δ_s at the corresponding values of ν . Results in the table are for Δ_s (in Kelvin) together with the gap predicted for homogeneous systems, Δ_h , and the saddle point width at the average saddle-point, a (in nm).

dependence of $\delta\phi$, and therefore b , on \sqrt{B} for states at ν as $\nu \rightarrow 1/2$, consistent with what we find. In Figs 2 and 3, we only show results for $\Delta_i/\Delta_s \gtrsim 0.2$ corresponding to $(a/\ell_q) \gtrsim 0.7$. For small a , the neglect of LL mixing in the WKB calculation is no longer justifiable, and there may also be direct tunnelling between QH-rich and QP-rich regions. Enhanced tunnelling would appear as a reduced value for a and may explain its low value at $\nu = 5/11$.

The microscopic gaps, Δ_s , computed using our model from the data of [4] are around 55% of the values, Δ_h , predicted using exact diagonalizations of systems of finite numbers of particles at $\nu = 1/3, 2/5, 3/7$, and 40% at $4/9$. Although the calculations take account of the nonzero width of the quantum wells and (perturbatively) of LL mixing, they are all for homogeneous systems. Residual short-range scatterers, omitted from our model, may lead to a reduction of the mobility gap [12, 13]. Furthermore, the presence of metallic screening regions makes it unlikely that Δ_h would be the correct value for Δ_s . First, Δ_h is the energy to create a QP or QH pair at infinite separation, while the excitations can be at most $O(a)$ apart across a saddle. Second, the interaction between particles, responsible for the gap in the incompressible regions in fractional quantum Hall systems, will be reduced by the screening of the nearby metallic regions. Although this screening will affect the form of the interaction, its principal effect in the lowest LL will be to reduce the overall strength of the interaction. A reduction of the gap by a factor which is roughly constant is reasonable.

We have analyzed the even-denominator states in the second LL using data taken at zero tilt angle on the sample discussed in Chapter 5 of [5]. This has $n =$

$1.6 \times 10^{11} \text{cm}^{-2}$ and $d = 160 \text{nm}$. We have extracted Δ_i/T_i from the Arrhenius plots and estimated the saddle-point gaps, Δ_s and (using $l_q = 2l_0$, $q = 1/4$) widths, a :

ν	Δ_i/T_i	$\Delta_i[\text{K}]$	$\Delta_s[\text{K}]$	$\Delta_h[\text{K}]$	a/l_q
5/2	5.4	0.32	0.40	1.0	1.7
7/2	1.0	0.035	0.14	0.85	0.84

The Δ_h have been computed for the spin-polarized ground states in a quantum well with the same density and well width (40nm) using exact diagonalization for small systems and accounting for LL mixing using the RPA method of [6]. For $\nu = 5/2$, $\Delta_s/\Delta_h \approx 0.4$, which is the same as that found for the state at $\nu = 4/9$ for the sample of [4] (see Fig. 3). For $\nu = 7/2$, the strong tunneling across the saddle point, $a/l_q \lesssim 1$, may explain the small Δ_s/Δ_h . We note that, according to our model, the quality of this sample is in part due to its large setback distance $d = 160 \text{nm}$. A large value of d will reduce the gradients of the impurity potential and hence lead to increased values for a . According to our model, even a small reduction in a would mean the loss of activated behavior at $\nu = 7/2$ in this sample.

Data for the integer quantum Hall effect (IQH) can also be accounted for on the basis of thermally assisted tunnelling. However, the IQH is more complicated, because the charging energy of a localized region $\sim (qe)^2/\epsilon d$ which in the fractional quantum Hall case is much smaller than Δ_s and which we have neglected, is larger and is likely to be important. Nevertheless, our analysis of the data of [9] shows that for the sample G160 Δ_i/T_i varies between nine at $\nu = 2$ ($\Delta_i/\Delta_s \approx 0.9$) and four ($\Delta_i/\Delta_s \approx 0.65$) at $\nu = 14$. For these filling fractions, T_u/T_d reduces from just over 2 ($\nu = 2$) to around 1.5 ($\nu = 14$) consistent with the prediction of our model [Fig. 2(b)].

Our adaptation of the model of [8], which takes account of the nucleation of carriers as a result of long-range potential fluctuations and of tunneling through saddle points, accounts for experimental data taken on fractional quantum Hall samples. The dissipative transport is controlled by the energy to create excitations close to a saddle point, Δ_s . This is smaller than the gap in an ideal homogeneous system, Δ_h , because of residual short-range scatterers and because of the changed nature of the interaction in the presence of nearby metallic screening regions. The gap extracted from Arrhenius plots, Δ_i , is reduced from Δ_s by tunneling effects by an amount that can be estimated via the ratio Δ_i/T_i (see Fig. 3). For a given filling fraction, the largest values of Δ_i will be observed in samples with small gradients of the disorder potential acting on the 2DEG. This will act to increase

typical saddle-point widths, a , and will occur in samples with large setback distances, d , and with the most even distribution of the ionized donors (thought to be enhanced by thermal cycling [5]), both of which lead to larger values of a .

We thank R.N. Bhatt for helpful remarks and G. Gervais for help with [5, 7]. The work was supported in part by the NSF under Grant DMR-0906475.

-
- [1] R. B. Laughlin, Phys. Rev. B, **23**, 5632 (1981).
 - [2] R. B. Laughlin, Phys. Rev. Lett., **50**, 1395 (1983).
 - [3] R. L. Willett, H. L. Stormer, D. C. Tsui, A. C. Gossard, and J. H. English, Phys. Rev. B, **37**, 8476 (1988).
 - [4] R. R. Du, H. L. Stormer, D. C. Tsui, L. N. Pfeiffer, and K. W. West, Phys. Rev. Lett., **70**, 2944 (1993).
 - [5] C. R. Dean, *A study of the fractional quantum Hall energy gap at half filling*, Ph.D. thesis, McGill (2009), digitool.library.mcgill.ca:8881/dtl_publish/4/40784.html.
 - [6] R. H. Morf and N. d'Ambrumenil, Phys. Rev. B, **68**, 113309 (2003).
 - [7] C. R. Dean, B. A. Piot, P. Hayden, S. Das Sarma, G. Gervais, L. N. Pfeiffer, and K. W. West, Phys. Rev. Lett., **100**, 146803 (2008).
 - [8] D. G. Polyakov and B. I. Shklovskii, Phys. Rev. Lett., **74**, 150 (1995).
 - [9] R. G. Clark, J. R. Mallett, S. R. Haynes, J. J. Harris, and C. T. Foxon, Phys. Rev. Lett., **60**, 1747 (1988).
 - [10] Y. Katayama, D. C. Tsui, and M. Shayegan, Phys. Rev. B, **49**, 7400 (1994).
 - [11] R. G. Clark, S. R. Haynes, J. V. Branch, A. M. Suckling, P. A. Wright, and P. M. W. Oswald, Surf. Sci., **229(1-3)**, 25 (1990).
 - [12] X. Wan, D. N. Sheng, E. H. Rezayi, K. Yang, R. N. Bhatt, and F. D. M. Haldane, Phys. Rev. B, **72**, 075325 (2005).
 - [13] G. Murthy, Phys. Rev. Lett., **103**, 206802 (2009).
 - [14] A. L. Efros, Solid State Commun., **67**, 1019 (1988).
 - [15] F. G. Pikus and A. L. Efros, Phys. Rev. B, **47**, 16395 (1993).
 - [16] A. L. Efros, Phys. Rev. B, **45**, 11354 (1992).
 - [17] A. M. Dykhne, Sov. Phys. JETP, **32**, 63 (1971).
 - [18] With reduced drift velocities (due to screening) and Coulomb scattering off particles in the compressible regions as the dominant scattering mechanism, the condition for equilibration is more easily satisfied than in [8] (where phonon scattering is the dominant mechanism).
 - [19] H. A. Fertig and B. I. Halperin, Phys. Rev. B, **36**, 7969 (1987).
 - [20] A. Matthews and N. R. Cooper, Phys. Rev. B, **80**, 165309 (2009).
 - [21] R. H. Morf, N. d'Ambrumenil, and S. Das Sarma, Phys. Rev. B, **66**, 075408 (2002).
 - [22] B. I. Halperin, P. A. Lee, and N. Read, Phys. Rev. B, **47**, 7312 (1993).